Biochimica et Biophysica Acta 1807 (2011) 336–347

Contents lists available at ScienceDirect

Biochimica et Biophysica Acta

journal homepage: www.elsevier.com/locate/bbabio

Regulation of electron transport in C_3 plant chloroplasts *in situ* and *in silico*: Short-term effects of atmospheric CO_2 and O_2

Ilya V. Kuvykin [a], Vasily V. Ptushenko [b,c], Alexey V. Vershubskii [a], Alexander N. Tikhonov [a,c,*]

[a] Faculty of Physics, M.V. Lomonosov Moscow State University, Moscow 119992, Russia
[b] A.N. Belozersky Institute of Physico-Chemical Biology, M.V. Lomonosov Moscow State University, Moscow 119992, Russia
[c] N.M. Emanuel Institute of Biochemical Physics of the Russian Academy of Sciences, Moscow, Russia

ARTICLE INFO

Article history:
Received 24 September 2010
Received in revised form 8 December 2010
Accepted 22 December 2010
Available online 30 December 2010

Keywords:
Photosynthesis
Electron and proton transport
Regulation
EPR
PAM-fluorimetry
Mathematical modeling

ABSTRACT

In this work, we have investigated the effects of atmospheric CO_2 and O_2 on induction events in *Hibiscus rosa-sinensis* leaves. These effects manifest themselves as multiphase kinetics of P_{700} redox transitions and non-monotonous changes in chlorophyll fluorescence. Depletion of CO_2 and O_2 in air causes a decrease in linear electron flux (LEF) and dramatic lowering of P_{700}^{+} level. This is explained by the impediment to electron efflux from photosystem 1 (PS1) at low acceptor capacity. With the release of the acceptor deficit, the rate of LEF significantly increases. We have found that oxygen promotes the outflow of electrons from PS1, providing the rise of P_{700}^{+} level. The effect of oxygen as an alternative electron acceptor becomes apparent at low and ambient concentrations of atmospheric CO_2 ($\leq$0.06–0.07%). A decrease in LEF at low CO_2 is accompanied by a significant (about 3-fold) rise of non-photochemical quenching (NPQ) of chlorophyll fluorescence. Such an increase in NPQ can be explained by more significant acidification of the thylakoid lumen. This occurs due to lessening the proton flux through the ATP synthases caused by a decrease in the ATP consumption in the Bassham–Benson–Calvin (BBC) cycle. pH-dependent mechanisms of electron transport control have been described within the frames of our mathematical model. The model describes the reciprocal changes in LEF and NPQ and predicts the redistribution of electron fluxes on the acceptor side of PS1. In particular, the contribution of cyclic electron flow around PS1 (CEF1) and water–water cycle gradually decays during the induction phase. This result is consistent with experimental data indicating that under the steady-state conditions the contribution of CEF1 to photosynthetic electron transport in *Hibiscus rosa-sinensis* is insignificant ($\leq$10%).

1. Introduction

Elucidation of the mechanisms of electron transport control and adaptation of photosynthetic organisms to varying environmental conditions is a topical problem of biophysics and biochemistry of photosynthesis (see for review [1–12] and references therein). In photosynthetic systems of oxygenic type (cyanobacteria, algae and chloroplasts of higher plants), the flexibility of photosynthetic apparatus in response to environmental changes is achieved by several regulatory mechanisms. At the level of photosynthetic electron transport chain, a short-term regulation of photosynthesis involves (*i*) activation of the Bassham–Benson–Calvin (BBC) cycle enzymes [13–16]; (*ii*) redistribution of electron flows through different pathways (noncyclic/cyclic/pseudocyclic electron transport) [17–29]; (*iii*) redistribution of light quanta between PS2 and PS1 ("state 1" ↔ "state 2" transitions) [3,4,9]; (*iv*) modulation of the rate of electron transport between PS2 and PS1 [30–36], and (*v*) dissipation of excess energy in the light-harvesting antenna of PS2 [12,37–48]. The latter two processes are associated with the light-induced acidification of the thylakoid lumen. A decrease in the lumen pH is known to decelerate the plastoquinol (QH_2) oxidation by the cytochrome b_6f complex, which impedes the electron flow to P_{700}^{+} [31–36]. Acidification of the lumen also causes the protonation of the PsbS subunit of PS2 that triggers the dissipation of excess absorbed light energy as heat [37–40]. Short-term feedback control of photosynthesis also includes regulation of chloroplast gene expression (within minutes) in response to perturbations of the redox state of the plastoquinone pool [6,12] or temperature changes [41].

Abbreviations: PS1 and PS2, Photosystem 1 and Photosystem 2, respectively; P_{700}, primary electron donor of PS1; P_{680}, primary electron donor of PS2; ATP, adenosine triphosphate; ADP, adenosine diphosphate; P_i, inorganic phosphate; BBC, Bassham–Benson–Calvin cycle; b_6f, plastoquinone–plastocyanin–oxidoreductase (b_6f-complex); CEF1, cyclic electron flow around PS1; EPR, electron paramagnetic resonance; Fd, ferredoxin; LEF, linear electron flux; NPQ, non-photochemical quenching; Pc, plastocyanin; Q, plastoquinone; QH_2, plastoquinol; WWC, water–water cycle (pseudocyclic electron transport)

* Corresponding author. Faculty of Physics, M.V. Lomonosov Moscow State University, Moscow 119992, Russia. Tel.: +7 495 9392973; fax: +7 495 9328820.
E-mail addresses: an_tikhonov@mail.ru, an_tikhonov@physics.msu.ru (A.N. Tikhonov).

0005-2728/$ – see front matter © 2010 Elsevier B.V. All rights reserved.
doi:10.1016/j.bbabio.2010.12.012

The possibility of switching between alternate electron transport pathways provides efficient and well-balanced output of ATP and NADPH to satisfy the requirements of plant metabolism. According to resent estimates (see for review [5,8]), a liner electron flow (LEF) from water to $NADP^+$ ($H_2O \rightarrow PS2 \rightarrow PS1 \rightarrow NADP^+$) provides the formation of ATP and NADPH in the ratio 9:7. This value is insufficient to support CO_2 fixation in the BBC cycle, which requires the ratio ATP:NADPH = 9:6. In C_3 plants, under photorespiring conditions and nitrate assimilation to glutamate, the energy requirements for CO_2 fixation was estimates as ~1.43 ATP:NADPH [11], resulting in deficit of ~0.13 ATP molecules per NADPH molecule reduced by LEF [8]. The flexibility of electron transport pathways in chloroplasts helps to optimize the operation of the photosynthetic apparatus, providing the required ATP:NADPH ratio. Type I flexibility mechanism (according to terminology suggested by Kramer and co-workers [7–10]) is achieved by modulating the influx of protons into the lumen per $NADP^+$ reduced. This mechanism implies the contribution of cyclic electron flow around PS1 (CEF1) and/or water–water cycle (WWC) into generation of the proton motive force that would provide the formation of additional ATP molecules. CEF1 is known to operate in addition to LEF in cyanobacteria and C_4-plants [17]. In C_3 vascular plants, the situation with CEF1 is less resolved [21]. When molecular oxygen rather than $NADP^+$ acts as a terminal electron acceptor in PS1, it is eventually reduced to water during operation of WWC [25–28]. Although CEF1 and WWC do not reduce $NADP^+$, they contribute to generation of the transmembrane electrochemical gradient of protons needed for operation of ATP synthase complexes. Thus, the proper stoichiometric ATP:NADPH ratio of 3:2 required for the BBC cycle operation could be attained due to the coordinated operation of alternate pathways of electron transport. Type II mechanism is believed to be associated with changing the effects of proton flux through the ATP synthase, without altering the ATP:NADPH output ratio [8,9].

Data concerning the functional role of alternate electron transport pathways are controversial (see reviews [1,2,7,12–15] and references therein). Tagawa and collaborators [42] were among the first to obtain evidence for activation of cyclic photophosphorylation under anaerobic conditions. However, some observations suggest that the removal of oxygen inhibits, rather than stimulates, cyclic electron transport [43]. The physiological role of oxygen as an alternative electron acceptor in PS1 (the Mehler reaction) of C_3 plants *in vivo* remains a matter of discussion. According to some reports, WWC is of minor importance and contributes only about 10% of total electron flow between PS2 and PS1 (see for review [26–28,44]). Therefore, many authors suppose that the Mehler reaction has no principal role in the functioning of the photosynthetic machinery in C_3 plants. However, there is another view on the role of oxygen in plant metabolism. For instance, oxygen is required for activation of Rubisco [45]. There is evidence that WWC can serve as a starter initiating energy-dependent events during the induction phase of photosynthesis [26]. It is supposed that the electron efflux from PS1 to oxygen prevents excessive accumulation of reduced electron carriers on the acceptor side of PS1 [24–27,44]. According to various estimates (see reviews [5,7,8]), the required ATP:NADPH ratio can be achieved if the electron flux diverted to CEF1 and oxygen constitutes a minor fraction, even as small as 10-15% of LEF. The relative contribution of WWC may vary depending on physiological factors. For example, the electron flows related to CO_2 and O_2 reduction in C_3 plants are redistributed upon lowering of leaf water content [21,46].

Among the diversity of short-term regulatory processes that serve to optimize photosynthesis, noteworthy are the mechanisms associated with light-induced changes in the lumen pH (pH_i) and stroma pH (pH_o). Modulation of pH_i is one of main factors controlling the rate of electron flow between PS2 and PS1. The lowering of pH_i slows down electron transfer at the cytochrome b_6f segment of electron transport chain (phenomenon known as photosynthetic control [31–36]). Another important regulatory mechanism, preventing over-excitation of PS2 and excessive acidification of the lumen, is the enhancement of energy dissipation in the light-harvesting antenna of PS2. This results in increased non-photochemical quenching (NPQ) of chlorophyll fluorescence [11,37–40]. Another aspect of pH-dependent regulation of electron transport is associated with the light-induced modulation of stroma pH_o. It is well-known that induction phenomena in photosynthetic systems are determined to a great extent by the light-induced activation of the BBC cycle that ensure carbon dioxide fixation at the expense of NADPH and ATP [1]. Along with the redox-dependent modulation of the BBC enzymes via the thioredoxin/thioredoxin-reductase system [47], the light-induced rise of stromal pH is also considered as one of the crucial factors that initiates the BBC cycle activation [1,13].

The mechanisms of electron transport control briefly considered above provide metabolic stability of photosynthetic apparatus upon fluctuations of environmental conditions, e.g., variations of atmospheric gases. Fluctuations in concentrations of CO_2 and O_2 around photosynthesizing leaves are well recognized. According to [48], oscillations of ambient atmospheric CO_2 concentration lasting for a minute or longer at low O_2 level (in order to eliminate photorespiration) may alter *in vivo* rate of LEF and photosynthetic CO_2 uptake in wheat leaves. De-aeration of the leaf atmosphere [49,50] and depletion of oxygen in the suspension of cyanobacterial cells due to respiration [51,52] have an essential impact on photosynthetic electron transport.

The aim of this study is to examine the influence of terminal electron acceptors (CO_2 and O_2) on the light-induced regulation of photosynthetic processes in *Hibiscus rosa-sinensis* leaves. Effects of illumination prehistory and concentrations of CO_2 and O_2 on photosynthetic electron transport have been investigated. Experimental data are analyzed within the frames of our mathematical model of electron and proton transport processes in chloroplasts.

2. Materials and methods

2.1. Plant material

Mature leaves of a room plant *Hibiscus rosa-sinensis* were used for EPR and fluorescence study of electron transport in chloroplasts *in situ*. Plants were grown in soil under natural lighting at day/night temperatures in the interval 20–24 °C and ~70–80% relative humidity. Our choice of *Hibiscus rosa-sinensis* as C_3 plant is explained by the following reasons. This plant has tough leaves of regular shape convenient for studding photosynthetic electron transport by the EPR and PAM-fluorimetry methods. Our experiments demonstrated that cuttings of *Hibiscus rosa-sinensis* leaves survived after several turns of short-term changes in CO_2 and/or O_2 concentrations in gas phase. Reproducible results were obtained after several cycles of illumination (see Fig. 8 and other details in Section 4.2).

2.2. Control of gas composition

During EPR measurements, a sample was positioned inside a quartz tube where the gas composition was controlled by pumping a mixture of gases containing molecular oxygen (O_2), carbon dioxide (CO_2), and neutral gas (N_2 or Ar) in various proportions. For chlorophyll fluorescence measurements, a portable fluorimeter with an attached leaf sample was placed into a special housing with controlled gas composition. The gas streams passing through a quartz tube positioned in the cavity of the EPR spectrometer, or passing through the fluorimeter housing, were finely adjusted by flow control valves inserted in the path between the gas tanks and the measuring equipment. In order to avoid drying artifacts owing to fanning the samples, a mixture of gases was moistened by passing through a vessel filled with distilled water. Concentrations of O_2 and CO_2 were

monitored with gas analyzers Klever-V (Delta Pro, Russia) and C2000 (Oldham, France), respectively.

2.3. EPR measurements of P_{700} redox transients

For EPR measurements, freshly cut segments of leaves (3 × 30 mm) were placed in a transparent plastic holder freely admitting atmospheric air or surrounding artificial mixture of gases. The holder with the specimen was placed into a quarts tube positioned at the center of the rectangular resonator of the Varian E-4 spectrometer (X-band). EPR signal attributed to oxidized centers P^{+}_{700} was registered at microwave power 10 mW and high-field modulation amplitude 4 G. To record the light-induced redox transients of P_{700}, the magnetic field was fixed at the low-field peak of the first derivative of the EPR signal. The time constant was 0.1 s. Specimens inside the resonator were illuminated with white light from a 100 W incandescent tungsten lamp focused on the resonator window. Infrared radiation was cut off with a 5-cm thick water filter. Actinic light intensity on the specimen surface was 320 W/m^2.

To standardize the experimental conditions, a sample placed into the EPR spectrometer cavity was first illuminated with white light for 1 min and then adapted to darkness for 10 min (unless otherwise specified). Following this pre-treatment, we then recorded the kinetics of light-induced changes in the amplitude of the EPR signal from P^{+}_{700}. All EPR measurements were performed at room temperatures (22–24 °C).

2.4. Leaf chlorophyll fluorescence measurements

Chlorophyll fluorescence in leaves was measured with a portable pulse amplitude modulation (PAM) fluorimeter (FluorPen FP100, Photon Systems Instruments, Czech Republic). This instrument is devised for measurements of fast fluorescence transients (*O-J-I-P* kinetic curve), as well as for determination of non-photochemical fluorescence quenching according to the commonly accepted illumination protocol for PAM-fluorimetry [37]. The excitation light had maximal intensity at 475 nm, spectral half-width 25 nm. In recording the non-photochemical quenching of chlorophyll fluorescence, saturating pulse power was 3000 μE·m^{-2}·s^{-1} (760 W/m^2), intensity of continuous actinic light was 300 μE·m^{-2}·s^{-1} (76 W/m^2). Probing pulses of 900 μE·m^{-2}·s^{-1} (230 W/m^2) followed at 1-s intervals. Fast fluorescence transients (*O-J-I-P*) were induced by light pulses followed at sampling intervals varying from 10 μs to 10 ms. Fluorescence measurements were performed on freshly cut leaf segments (10 × 10 mm) attached to the fluorimeter placed into a camera with controlled gas composition. All fluorescence measurements were performed at room temperatures (22–24 °C).

2.5. Fluorescence parameters and rate constants

Chlorophyll fluorescence measurements provide a means to quantify the efficiency of photochemical processes as well as heat dissipation of absorbed light energy in chloroplasts. PAM-fluorometry allows researchers to separate the contributions of photochemical and non-photochemical fluorescence quenching [37–40]. Fig. 1 shows typical changes in chlorophyll fluorescence in *Hibiscus rosa-sinensis* leaves as measured with conventional PAM-fluorimetry protocol. Arrows indicate the moments when saturating light pulses were applied either in darkness or on the background of continuous actinic light. The F^0_m value designates the maximum yield of fluorescence induced by the first saturating pulse in a dark-adapted leaf. After switching on continuous actinic light, fluorescence first increases rapidly and then diminishes slowly. Such non-monotonic time pattern, often termed 'slow fluorescence induction', has long been known as the Kautsky effect [1,53]. In line with a slow decline of fluorescence, the fluorescence level $F'_m(t)$, probed by saturating pulse

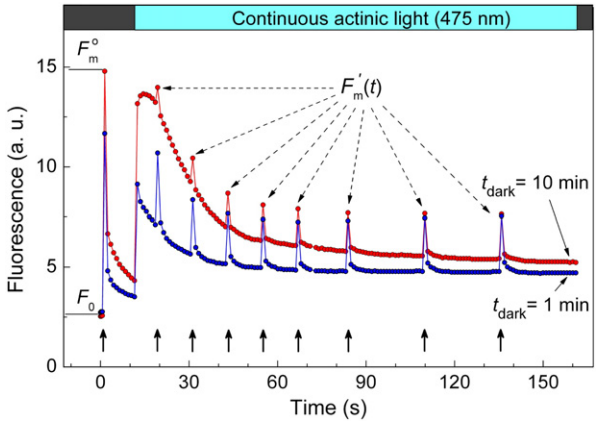

Fig. 1. Light-induced changes in chlorophyll fluorescence in dark-adapted *Hibiscus rosa-sinensis* leaves exposed to the treatment with saturating light pulses (indicated by vertical arrows) and continuous actinic light used for assaying non-photochemical fluorescence quenching. Prior to the application of first saturating light pulse, pre-illuminated leaf was adapted to the dark for 10 or 1 min, as indicated.

at appropriate time moment *t*, also lowers. This reflects a decrease in quantum yield of chlorophyll fluorescence caused by the enhancement of NPQ. The extent of NPQ measured at given moment of time *t* is quantified with the q_{NPQ} value [37,40]:

$$q_{NPQ}(t) = \frac{F^0_m - F'_m(t)}{F'_m(t)} \quad (1)$$

Parameter q_{NPQ} measures changes in heat dissipation of energy in the light-harvesting antenna of PS2 relative to initial dark-adapted state [37,40]. The dominant contribution to NPQ gives so-called 'high energy state quenching' (often reported as q_E) associated with chloroplast energization caused by acidification of the thylakoid lumen. The contribution of a 'state transition quenching' (q_T) to NPQ, associated with the energy redistribution between PS2 and PS1, is usually small and manifests itself only at low intensity illumination [40].

Another fluorescence parameter used to quantify electron flux through PS2 is the Φ_{PS2} value (often termed as "PS2 operating efficiency" [37,40]) determined as

$$\Phi_{PS2} = \frac{F'_m(t) - F(t)}{F'_m(t)} \quad (2)$$

Here, $F(t)$ stands for fluorescence intensity measured immediately before the action of saturating pulse given at the time moment *t*. Parameter Φ_{PS2} (also designated as F'_q/F'_m or $\Delta F/F'_m$ [37,40]) characterizes the quantum yield of PS2 photochemical activity. It has been suggested to use parameter Φ_{PS2} for measuring LEF in chloroplasts *in vivo* [37,40]:

$$J_{LEF} = PPFD \cdot \alpha_2 \cdot \Phi_{PS2} \quad (3)$$

where *PPFD* is the photosynthetically active photon flux density (μmol photon·m^{-2}·s^{-1}) of absorbed light and α_2 is a partitioning factor that accounts for the energy distribution between PS2 and PS1.

To characterize photosynthetic activity of chloroplasts, we also used the photochemical quenching parameter q_p, which is the current proportion of open PS2 centers [37,40]. Parameter q_P was calculated according to [54] as the following term

$$q_P = \frac{F'_m(t) - F(t)}{F'_m(t) - F_0 / ((F^0_m - F_0)/F_m + F_0/F'_m(t))} \quad (4)$$

3. Mathematical modeling of electron and proton transport

For quantitative analysis of experimental data, we simulated the light-induced processes in chloroplasts within the framework of a mathematical model developed previously [55–65]. This model considers the key steps of photosynthetic electron and proton transfer, the trans-thylakoid proton transport coupled to ATP synthesis (Fig. 2) and proton exchange between the lumen, stroma and cytoplasm (see Supplementary data). Numerical experiments were run to describe the light-induced redox transients of electron carriers P_{700}, P_{680}, plastoquinone (Q), plastocyanin (Pc), ferredoxin (Fd), NADP, as well as ATP synthesis and pH changes in the chloroplast lumen (pH_i) and stroma (pH_o).

3.1. Electron transport processes

The scheme of electron transport processes under consideration (Fig. 2) includes the main stages of electron transfer in thylakoids. The model takes into account three alternative pathways of electron outflow from PS1. The first one is associated with the noncyclic electron flow from PS2 to $NADP^+$ ($H_2O \rightarrow PS2 \rightarrow Q \rightarrow PS1 \rightarrow Fd \rightarrow NADP^+$) which produces NADPH. The terminal two-electron acceptor $NADP^+$ is localized in stroma. NADPH serves as a hydrogen donor in the BBC cycle. The second pathway is a 'short' cyclic electron flow around PS1 (CEF1) that returns electrons to the electron transport chain in the region between PS2 and PS1. In this way, electrons from reduced Fd molecules are delivered to the plastoquinone pool without the $NADP^+$ reduction. The third path of electron outflow from PS1 is associated with the Mehler reaction (electron transfer from Fd to O_2).

Our model describes the light-induced generation of a trans-thylakoid pH difference ($\Delta pH = pH_o - pH_i$) which is the driving force for ATP synthesis by the membrane-bound F_0F_1-ATP synthase. Consumption of ATP and NADPH in the BBC cycle is also taken into consideration. The model envisages pH-dependent activation of the BBC cycle reactions upon the light-induced alkalization of stroma (see [62,64,65] and Supplementary data for details).

3.2. Proton transport processes

Within the frames of our model, protons accumulate inside the thylakoid owing to light-induced splitting of water in PS2 and plastoquinol (QH_2) oxidation by the b_6f complex (see Fig. 2 and Fig. 1A in Supplementary data). Protons drain from the lumen in two ways: (*i*) via the F_0F_1-ATPsynthase (proton flux J_{ATP} coupled to ATP synthesis), and (*ii*) by passive leakage (proton flux J_{pass}). ATP-dependent proton flux J_{ATP} is a function of variables $[H^+_i]$ and $[H^+_o]$, the lumenal and stromal concentrations of hydrogen ions, and ATP concentration in stroma (see Supplementary data and [65]). Passive proton flux J_{pass} is independent of [ATP]. The model also takes into account the proton exchange between stroma and cytosol (proton flux J_{cyt}). The value of pH in the cytoplasm is taken to be constant ($pH_{cyt} = 8.0$) owing to a high buffer capacity of the cytosol. Algebraic functions describing proton fluxes were described earlier (see original works [55–66] and appropriate comments in Supplementary data).

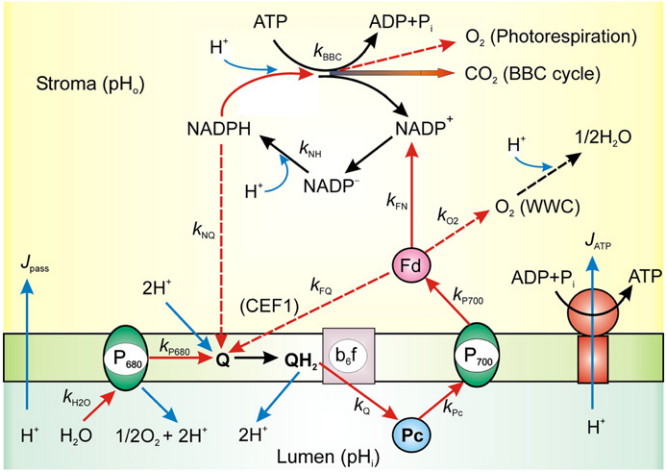

Fig. 2. Scheme of electron and proton transport processes considered in the model.

3.3. Electron fluxes, rate constants, model parameters and computation details

The apparent rate constants for partial reactions of electron and proton transport were determined by fitting respective experimental and simulated kinetic curves as described earlier (see [65] and references therein). Effects of pH-dependent down-regulation of PS2 photochemical activity and electron transfer rate from PS2 to P^+_{700} were modeled as described in [65]. Plastoquinol oxidation by the b_6f complex is the rate-limiting step in the electron transport chain between PS2 and PS1. The influence of pH_i on this reaction is described in [65] (see Supplementary data for computational details). To model effects of non-photochemical dissipation of energy in PS2, parameter L_2 (a number of light quanta exciting P_{680} per unit time) was set as a phenomenological sigmoid function $L_2(pH_i)$ which value decreased with the lumen acidification [64,65].

Partial electron fluxes from PS1 to $NADP^+$ (J_{BBC}), to oxygen (J_{O2}), and cyclic electron flux around PS1 (J_{CEF1}), as well as NADPH and ATP consumption in the BBC cycle were calculated as described in Supplementary data. Differential equations for the description of redox transients of electron carriers, pH changes, ATP synthesis and ATP consumption, are listed in the Supplementary data. The choice of effective rate constants and parameterization of pH-dependent electron transport processes are detailed in [65].

4. Results and discussion

4.1. Effect of atmospheric O_2 and CO_2 on light-induced redox transients of P_{700}

4.1.1. Effects of illumination prehistory

Photosynthetic electron transport depends on illumination prehistory. This phenomenon is termed in general as 'induction phenomenon' [1,53]. Electron paramagnetic resonance (EPR) is a convenient means to study induction phenomena in optically dense specimens, higher plant leaves in particular. The EPR method is readily suitable for monitoring the redox state of PS1 reaction centers P_{700}. Fig. 3A shows EPR spectra of *Hibiscus rosa-sinensis* leaves in darkness and in light, as indicated. The light-induced EPR signal has a peak-to-peak width of $\Delta H_{pp} \approx 8$–9 G. This signal is attributed to the ion-radical P^+_{700} of PS1 [67].

Fig. 3B shows typical patterns of P_{700} photooxidation in dark-adapted leaves. Before the EPR measurements, each sample was pre-illuminated for 1 min with the white light (WL) and then was adapted to the dark. As one can see, after sufficiently long dark adaptation ($t_{ad} \geq 1$–5 min), the kinetics of P_{700} photooxidation was clearly multi-phasic. A comparatively small (10–20%) initial jump of the EPR signal (stage *A*) was followed by a short lag phase and subsequent *S*-shaped signal increase (stage *B*). The duration of the lag phase preceding the signal rise in phase *B* increased with the adaptation time. The third distinct phase (stage *C*) was manifested as a comparatively slow ($\tau_{1/2} \sim 30$–60 s) increase in the EPR signal. After ceasing the illumination, the EPR signal returned to its initial level. Repeated illumination after a short dark period (≤ 30 s) resulted in fast monotonous oxidation of P_{700}. In this case, the separation between phases *A*, *B* and *C* disappeared.

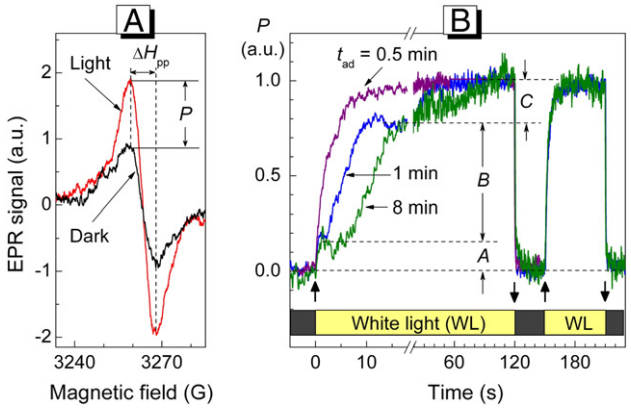

Fig. 3. EPR spectra of *Hibiscus rosa-sinensis* leaves measured in dark and in light as indicated (A), and kinetics of light-induced changes in the amplitude of the EPR signal from P_{700}^{+} (B). After 1-min pre-illumination with white light, samples were adapted for 0.5, 1, or 8 min to the dark, as indicated.

Fig. 4 illustrates how the induction phase, characterized by parameter $\tau_{1/2}$ (the half-time of the kinetic phase *B*), depends on the dark adaptation time, t_{ad}. It can be seen that the dark adaptation interval of 8–10 min is sufficient for relaxation to the 'dark-adapted state' routinely used in this work to standardize a state of pre-illuminated sample before the EPR and fluorescence measurements. Note that the distinctions in kinetic behavior of P_{700} in dark-adapted and pre-illuminated leaves could be caused by de-energization of chloroplasts in darkness (dissipation of ΔpH) and adaptive changes in the photosynthetic apparatus [1]. For example, the BBC cycle metabolites might be present in larger amounts in pre-illuminated samples (these metabolites can persist for long periods in darkness [1]), thus favoring a faster activation of the BBC cycle. The discussion of this topic goes beyond the scope of the present article. However, we have to emphasize that induction effects should be taken into account for correct standardization of experimental conditions in studies with intact photosynthetic systems.

4.1.2. Effect of O_2 and CO_2 on photooxidation of P_{700}

Electron transport in *Hibiscus rosa-sinensis* leaves strongly depends on the presence of oxygen and CO_2. Fig. 5 shows how a steady-state level of P_{700}^{+} gradually decreases with depletion of O_2 in air surrounding a sample. In this experiment, a specimen (a cut-out piece of the leaf placed into a cavity of the EPR spectrometer) was blown with a mixture of N_2 and O_2 gases. In de-oxygenated samples

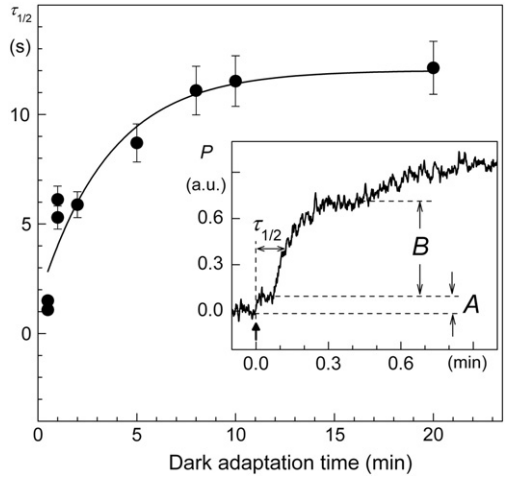

Fig. 4. Dependence of the induction phase parameter $\tau_{1/2}$ (the half-time of phase B in the kinetics of P_{700} photooxidation) on the dark adaptation time.

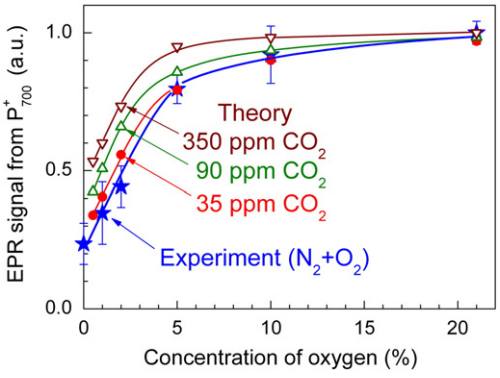

Fig. 5. Effects of atmospheric oxygen on the steady-state amplitude of the EPR signal from oxidized centers P_{700}^{+} in *Hibiscus rosa-sinensis* leaves (denoted by stars, $n = 4–7$, vertical bars are SE) or calculated within the frames of the model for various concentrations of CO_2 (denoted by solid circle, and up and down triangles, as indicated).

([O_2]<0.5%), a level of photooxidized centers P_{700}^{+} was insignificant, being comparable to the first phase of P_{700} oxidation (phase *A*) observed under aerobic conditions ([O_2] = 21%). The strong depression of P_{700}^{+} level under anaerobic conditions can be explained, at least partly, if we consider oxygen as an alternative electron sink in PS1 [24–28,50-52]. The deficit of oxygen would result in accumulation of reduced electron carriers on the acceptor side of PS1. The "over-reduction" of PS1 acceptors should prevent P_{700} photooxidation.

There are clear indications that the strong decrease in P_{700}^{+} level, observed after relatively short-term (~5–10 min) blowing of samples with N_2 gas, is associated with the removal of oxygen, but not only due to depletion of endogenous CO_2. Actually, the leaves incubated in the atmosphere of O_2 and N_2 (21% O_2 without CO_2) displayed practically the same steady-state level of P_{700}^{+} (Fig. 6, column 4) as that

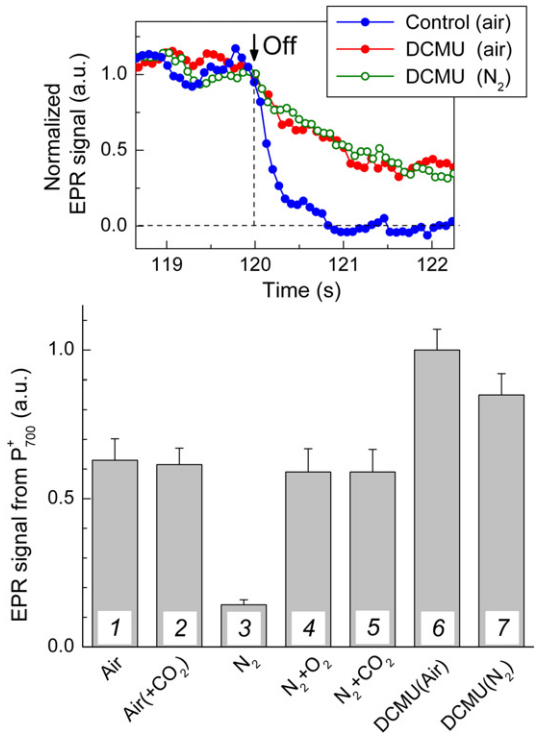

Fig. 6. Effects of atmosphere gas composition on the steady-state level of P_{700}^{+} (columns 1–7 in the bottom panel). The upper panel shows the post-illumination kinetics of P_{700}^{+} reduction in control and DCMU-treated leaves. Concentration of O_2 in experiments corresponding to columns 1, 2, 4, and 6 was 21%. Concentration of CO_2 in experiments corresponding to columns 2 and 5 was 1%.

observed in the samples incubated in the air (Fig. 6, column 1) or in the air with the elevated content of CO_2 (Fig. 6, column 2). It should be noted that a shortage of O_2 can be compensated by high atmospheric CO_2, the physiological sink of electrons in PS1 (Fig. 6, column 5). All these observations indicate that a significant decrease in the P^+_{700} level in the leaves exposed to N_2 gas (Fig. 5) resulted from the removal of O_2, but not merely from the depletion of endogenous CO_2. This conclusion finds another support from the measurements of chlorophyll fluorescence (Section 4.2.) and theoretical modeling of the plot of $[P^+_{700}]$ versus O_2 concentration at different partial pressures of atmospheric CO_2 (Fig. 5).

Note that a decrease in the level of P^+_{700} under the low electron acceptor conditions could be determined, in principle, by two factors: (*i*) an impediment to electron outflow from PS1, and (*ii*) an acceleration of electron input to P^+_{700}. As one might expect, a deceleration of LEF under the low acceptor capacity conditions would slow down the operation of proton pumps, resulting in a decrease in ΔpH. This in turn would accelerate electron flow from PS2 to PS1. However, PAM-fluorimetry data (Section 4.2), as well as our numerical experiments (Section 4.3), showed that this was not the case.

Another possible reason for reducing the steady-state level of P^+_{700} at low capacity of electron acceptors might be associated with redox-dependent activation of CEF1 [68–70]. Oxygen-dependent electron fluxes to P^+_{700} from endogenous donors (e.g., reduced metabolites in chloroplasts and mitochondria) could also influence a level of P^+_{700}. In order to examine possible effects of O_2 depletion on CEF1, we have compared the control samples with leaves infiltrated with 0.1 mM DCMU (3-(3',4'-dichlorophenyl)-1,1-dimethylurea) solution. At this concentration, DCMU completely inhibits PS2 activity. Therefore, only CEF1 and/or endogenous reductants other than PS2 could donate electrons to P^+_{700} centers. In DCMU-treated samples, the steady-state level of P^+_{700} was markedly higher than in control samples (leaves infiltrated with physiological solution without DCMU) (cf. columns *1* and *6* in Fig. 6). As one can see from the upper panel in Fig. 6, the post-illumination reduction of P^+_{700} in DCMU-treated leaves takes much longer time ($\tau_{1/2}$ ~ 1 s) than in control samples ($\tau_{1/2} \leq$ 100 ms, see also [71]). This data imply that in DCMU-treated leaves the electron flux to P^+_{700} is negligible as compared with control (untreated) leaves. Therefore, we can conclude that under the steady-state conditions CEF1 and endogenous electron donors give insignificant contribution to P^+_{700} reduction as compared with the electron flux from PS2. These data are consistent with the reports that in C_3 vascular plants steady-state CEF1 *in vivo* constitutes ≤10–15% of steady-state LEF (see for review [8–10,17]).

It should be noted that photooxidation of P_{700} is sensitive to oxygen depletion even in DCMU-treated leaves (cf. columns *6* and *7* in Fig. 6). This result might be interpreted in a way that the removal of oxygen promotes CEF1, thus lowering the level of P^+_{700}. However, this is not the case, because the post-illumination reduction of P^+_{700} in DCMU-treated samples was the same in the air and in O_2-free environment (Fig. 6, upper panel). This result indicates that electron supply to P^+_{700} from cyclic pathway and/or endogenous donors remained slow under anaerobic conditions. Note that in O_2-free atmosphere DCMU-treated samples revealed significantly higher level of P^+_{700} than in aerated control leaves (cf. columns *1* and *7* in Fig. 6). We assume that a decrease in the light-induced signal of P^+_{700} with the depletion of O_2 in DCMU-treated leaves (cf. columns *6* and *7* in Fig. 6) is explained mainly by the hindrance to electron outflow from PS1, but not due to acceleration of electron input to P^+_{700} via CEF1. Thus, we conclude that under aerobic conditions oxygen promotes the outflow of electrons from PS1, releasing the over-reduction of the acceptor side of PS1.

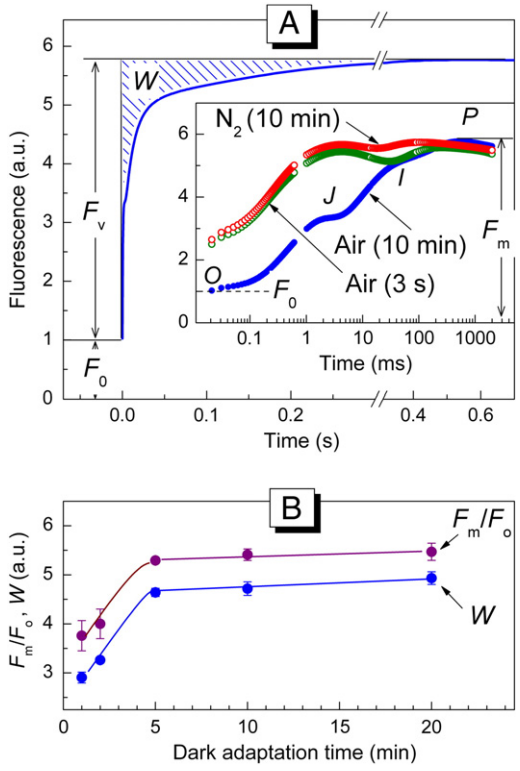

Fig. 7. Fast transients (*O-J-I-P* curve) of the chlorophyll fluorescence in *Hibiscus rosa-sinensis* leaves adapted to darkness in air (for 10 min or 3 s) or in nitrogen (for 10 min) atmosphere (A), and plots of the fluorescence parameters F_m/F_0 and *W* vs. the dark adaptation time, t_{ad}, for samples exposed to air (B).

4.2. Effect of atmospheric O_2 and CO_2 on chlorophyll fluorescence

4.2.1. Effects of pre-illumination history on the O-J-I-P curve

A fluorescence induction curve (*O-J-I-P*) provides information on the redox state of the chloroplast electron transport chain. Fig. 7A compares the *O-J-I-P* curves in dark-adapted (10 min) samples exposed to air or to N_2 atmosphere. In control leaves, we observed typical multi-phasic induction curve characterized by the ratio $F_v/F_m \approx 0.83$, where $F_v = F_m - F_0$ is a variable component and F_m is a maximal level of fluorescence. This value is typical of F_v/F_m values in dark-adapted leaves of C_3 plants [72,73]. Repeated illumination of aerated sample after the short period of darkness ($t_{ad} = 3$ s) showed the ratio $F_v/F_m \approx 0.56$. This is because the short-term adaptation to the dark ($t_{ad} = 3$ s) is insufficient for oxidation of the plastoquinol pool in pre-illuminated chloroplasts [74,75]. In this case, the initial level of fluorescence, F_0, is markedly higher than after the long-term adaptation to darkness (t_{ad} ~ 10 min). Oxidation of QH_2 in the dark occurs by means of direct interaction with O_2 and/or via the chloroplast terminal oxidases [44]. Fig. 7B shows the plots of parameters F_m/F_0 and *W* versus the dark adaptation time for samples exposed to air. Parameter *W* (an area over the *O-J-I-P* curve, see Fig. 7A for definition), as well as the ratio F_m/F_0, can serve as a measure for oxidized plastoquinone pool [74,75]. One can see that 5-min dark adaptation ensures almost complete relaxation of chloroplasts to the state with oxidized plastoquinone pool. This is consistent with previously reported data for *Hibiscus rosa-sinensis* leaves [74].

Pre-illuminated samples adapted to darkness (10 min) in the O_2-free atmosphere showed significantly higher initial level of fluorescence (by a factor of 2.6) than aerated samples (Fig. 7A). The fluorescence rise time to maximal level F_m was significantly shorter than in aerated samples. This provides clear evidence that under anaerobic conditions the major part of electron carriers localized between PS2 and PS1 (plastoquinone pool) remained reduced even after sufficiently long (~10 min) adaptation. Note that the presence or absence of CO_2 in the N_2-flow did not influence a shape of the *O-J-I-P* kinetic curve (data not shown).

4.2.2. Photochemical and non-photochemical quenching of chlorophyll fluorescence

Fig. 8 presents the typical patterns of time-courses of fluorescence parameters Φ_{PS2}, q_P, and q_{NPQ} measured during several successive cycles of illumination. Samples were dark-adapted (10 min) under aerobic conditions prior to each illumination cycle. Curves 1, 2 and 4 correspond to the first, second and fourth cycles, respectively. Despite a general similarity between the corresponding kinetic curves, fluorescence transients slightly differed in response to the first (curve 1) and other cycles of illumination (curves 2, 4). Note that the difference between all the subsequent curves (cf. corresponding curves 2 and 4) was not essential. This circumstance is important for standardizing the protocol for assaying the effects of gases. Usually, we compared results of three consecutive measurements: *i*) kinetic curve obtained for dark-adapted (10 min) sample incubated in air (the second cycle of illumination); *ii*) kinetic curve for dark-adapted sample exposed to modified gas atmosphere (third cycle of illumination), and *iii*) the repetition of measurements on air-conditioned sample (forth cycle of illumination). Using this protocol, we could compare an experimental curve with the control ones measured before and after changes in gas atmosphere. The proximity of the kinetic curves for the second and fourth cycles of illumination we considered as a criterion for maintaining the sample intactness after changes in gas composition.

Fig. 9 shows the effects of O_2 and CO_2 on the time-courses of parameters Φ_{PS2} (Fig. 9A) and q_{NPQ} (Fig. 9B) in *Hibiscus rosa-sinensis* leaves. Parameter Φ_{PS2} is proportional to electron flux through PS2. Upon blowing a sample with N_2 gas ($[CO_2] << 0.005\%$; $[O_2] < 0.5\%$), we observed a significant decrease in the quasi-stationary level of PS2 operating efficiency ($\Phi_{PS2} < 0.03$). This indicates a low rate of LEF in deficiency of both PS1 acceptors, CO_2 and O_2. In the presence of one of these acceptors, either at 21% O_2 without CO_2 (curve '$N_2 + O_2$') or at ambient concentrations of CO_2 without O_2 (curve '$N_2 + CO_2$'), the quasi-stationary rate of LEF increased several times ($\Phi_{PS2} \approx 0.12$).

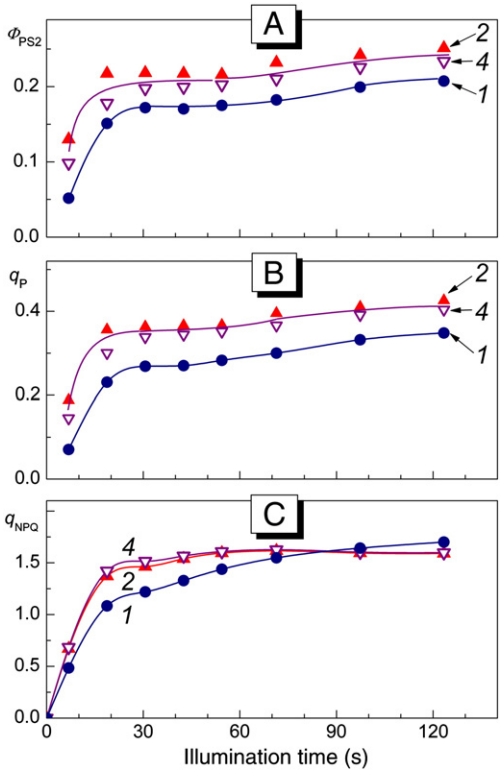

Fig. 8. Time-courses of the fluorescence parameters Φ_{PS2} (A), q_P (B), and q_{NPQ} (C) measured for several successive cycles of leaf illumination. Numbers at the curves denote the number of illumination cycle (see explanation in the text).

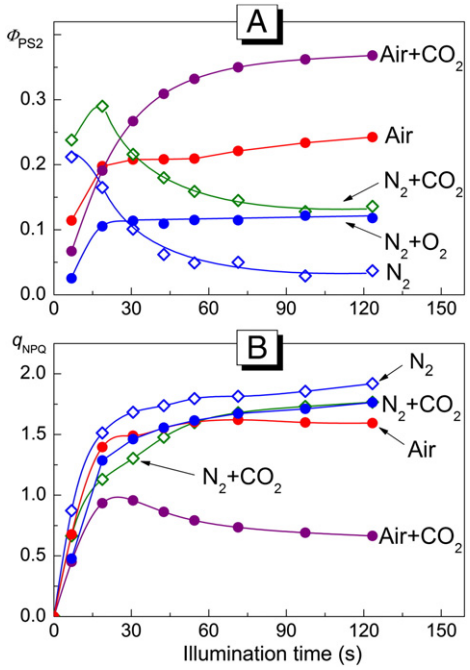

Fig. 9. Effects of atmospheric gas composition on the time-courses of the fluorescence parameters Φ_{PS2} (A) and *NPQ* (B) in *Hibiscus rosa-sinensis* leaves. During 10-min dark adaptation, a leaf was blown by the following gases: 1) N_2 ($[O_2] < 0.5\%$, $[CO_2] < 0.005\%$); 2) $N_2 + O_2$ ($[O_2] = 21\%$); 3) $N_2 + CO_2$ ($[O_2] < 0.5\%$, $[CO_2] = 0.11 \pm 0.01\%$); 4) Air; 5) Air + CO_2 ($[CO_2] = 0.15 \pm 0.05\%$).

Elevated LEF in CO_2-free air demonstrates that the water–water cycle ($H_2O \rightarrow PS2 \rightarrow PS1 \rightarrow O_2 \rightarrow H_2O$) can support sufficiently high electron transport even under the conditions unfavorable for operation of the BBC cycle. In the normal air atmosphere, the effects of CO_2 and O_2 are synergetic ($\Phi_{PS2} \approx 0.25$, curve 'Air'). With a significant rise of CO_2 ($[CO_2] \approx 1\%$, curve "Air + CO_2"), we observed a further increase in the operating efficiency of PS2 ($\Phi_{PS2} \approx 0.37$). Significant stimulation of LEF ($H_2O \rightarrow PS2 \rightarrow PS1 \rightarrow NADP \rightarrow CO_2$) at high concentrations of CO_2 is associated with the rise of the BBC cycle turnover. An increase in LEF in the presence of PS1 acceptors (Fig. 9A) correlates with a decrease in q_{NPQ} (Fig. 9B). Similar observation concerning the reciprocal behavior of LEF and NPQ at low acceptor power has been reported by Kramer and collaborators for *N. tabacum* leaves [76,77].

Fig. 10A compares the dependences of quasi-stationary parameter Φ_{PS2} on CO_2 concentration in air (at $[O_2] = 21\%$) and in O_2-free gas mixture ($N_2 + CO_2$). Both dependences show a monotonous rise of Φ_{PS2}, which value reaches a maximum magnitude at $[CO_2] \geq 0.1$–0.15%. At low and ambient concentrations of CO_2 (≤ 0.07–0.08%), one can notice a clear difference between aerated and de-aerated samples: the depletion of O_2 caused a decrease in Φ_{PS2}. Less significant but also clear difference between the aerated and O_2-free samples was also observed for parameter q_{NPQ} (Fig. 10B). At high concentrations of CO_2 ($\geq 0.1\%$), the differences between these samples disappeared.

Significant increase in Φ_{PS2} with the rise of PS1 electron acceptor capacity is not surprising. Interestingly that the acceleration of LEF is accompanied by a marked decrease in q_{NPQ} ($CO_2\uparrow \rightarrow LEF\uparrow \rightarrow NPQ\downarrow$), indicating a decrease in ΔpH at high concentrations of CO_2 ($\geq 0.15\%$). How could one explain a down-regulation of NPQ (Fig. 10B) with stimulation of LEF (Fig. 10A)? A decrease in the q_{NPQ} value certainly points to a decrease in ΔpH. Therefore, we cannot attribute this effect to acceleration of proton pumping into the lumen. Obviously, the intensification of LEF at high atmospheric CO_2 is accompanied by acceleration of the proton efflux from the lumen ($CO_2\uparrow \rightarrow LEF\uparrow \rightarrow \Delta pH\downarrow$). Actually, a fast rate of carbon assimilation will impose a considerable drain of NADPH and ATP. Acceleration of ATP utilization in the BBC cycle

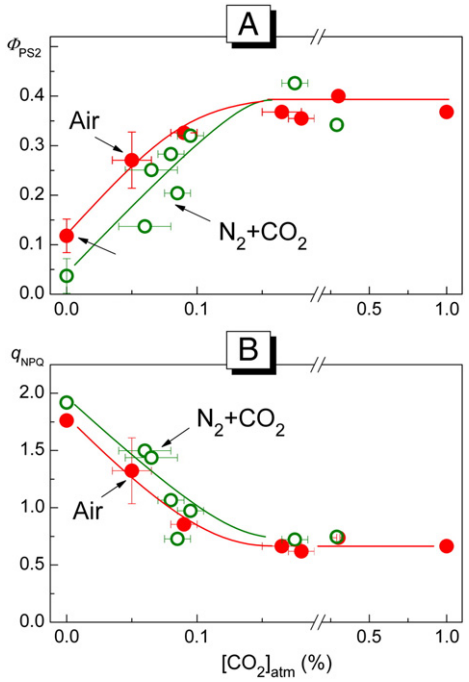

Fig. 10. Quasi-stationary values of the fluorescence parameters Φ_{PS2} (A) and q_{NPQ} (B) vs. the CO_2 concentration in the air or in O_2-free gas mixture ($N_2 + CO_2$). Horizontal bars indicate the intervals of variations of CO_2 level during the dark adaptation prior to fluorescence measurements.

would maintain high rates of ATP synthase turnover, thus lowering the ΔpH (BBC cycle↑ → ATP synthase↑ → ΔpH↓).

In the meantime, the rise of NPQ with a significant decrease in PS1 acceptor capacity cannot find simple mechanistic explanation. Actually, the turnover of proton pumps coupled to LEF would decelerate at low CO_2. The reciprocal behavior of LEF and NPQ at low CO_2 (CO_2↓ → LEF↓ → NPQ↑) indicates an increase in ΔpH. This effect might be explained, in principle, by the onset of CEF1 that would promote the proton pumping into the lumen. There is strong evidence for participation of CEF1 in ATP synthesis in green algae, cyanobacteria and in C_4 plants [17]. However, in C_3 vascular plants the relative contribution of steady-state CEF1 to proton flux do not change appreciably when CO_2 or when both CO_2 and O_2 concentrations are decreased, remaining at low level to account for a significant rise of NPQ (see for review [8]). According to our estimates (section 4.1), in *Hibiscus rosa-sinensis* leaves the proportion of CEF1 to steady-state electron influx to P_{700}^+ does not exceed 10–15%. To our opinion, a reasonable explanation of the up-regulation of NPQ is that a decrease in the ATP consumption at low atmospheric CO_2 leads to deceleration of the ATP synthase turnover. This will result in reducing the proton drain from the lumen to stroma and the elevation of NPQ (CO_2↓ → ATP synthase↓ → ΔpH↑ → NPQ↑). The same mechanism of up- and down-regulation of LEF and NPQ has been derived from our experiments *in silico* (section 4.3).

As one can see from Fig. 10, the depletion of O_2 at low and ambient concentrations of CO_2 causes a decrease in LEF (Fig. 10A) and a certain increase in NPQ (Fig. 10B). These effects can be explained by the Warburg effect in C_3 plants [1], i.e., due to enhancement of carbon assimilation under anaerobic conditions. Interestingly that even at very low electron acceptor capacity, when the leaf was placed in pure N_2 atmosphere (without CO_2 and O_2), the q_{NPQ} value was high enough (≈1.8–1.9). This result demonstrated that photosynthetic electron transport was maintained at the level sufficient to generate a high enough ΔpH. It should be emphasized that significant decrease in LEF observed upon flushing the leaf with N_2 (Fig. 9A) could not result exclusively from the depletion of endogenous CO_2. A reasonable explanation is that a short-term (~5–10 min) flushing of the sample with N_2 gas effectively removes oxygen from the leaf interior, but is insufficient for complete depletion of endogenous source of carbon (CO_2 and/or HCO_3^-) in the chloroplast stroma. As it was shown with oxygen-sensitive paramagnetic probes injected into bean leaves [78,79], the ventilation of the leaf interior was sufficient for maintaining the oxygen partial pressure at the atmosphere level, both in the dark or during the illumination of the leaf. Such a good ventilation of the leaf interior can be explained by rapid, long-distance diffusion of oxygen from chloroplasts to leaf stomata [78,79]. In O_2-free atmosphere containing ambient or low concentrations of CO_2, the efficiency of PS2 operation was markedly lower than in air (Figs. 9A and 10A). This means that oxygen acted as an efficient optional sink for electrons, helping to elevate the rate of electron transfer through PS1.

Concerning the role of oxygen as an alternative electron acceptor in chloroplasts, it is interesting to remember some circumstances noted in the recent work [80]. In chloroplasts, the concentrations of CO_2 and O_2 are below their K_M values for Rubisco (K_M = 9 μM for CO_2 and K_M = 535 μM for O_2 [81]). Owing to a high concentration of Rubisco active sites in chloroplasts (up to ~4−10 mM, in C_3 plants [82,83]) and low stromal concentration of CO_2 (~12 μM, in equilibrium with air at 25 °C), Rubisco should drastically deplete CO_2 in the vicinity of its active sites by keeping it bound in the enzyme-substrate complex. Roussel and Igamberdiev [80] argued in favor of a mechanism that should prevent the depletion of CO_2 in the vicinity of Rubisco below the range at which Rubisco is still operative. They suggested that the oxygenase reaction of Rubisco could prevent the CO_2 concentration from dropping below a certain minimum level.

4.3. In silico study of electron and proton transport control in chloroplasts

One of the factors controlling electron transport in chloroplasts is the light-induced acidification of the thylakoid lumen. A decrease in pH_i is known to decelerate the oxidation of QH_2 by the cytochrome b_6f complex, thus impeding electron flow from PS2 to PS1 [31–36]. Acidification of the lumen also causes the protonation of PsbS subunit of PS2 that triggers the dissipation of absorbed light energy as heat [38–40]. The chain of the feedback control of electron transport on the acceptor side of PS1 includes the processes of ATP and NADPH consumption in the BBC cycle. Results of our experiments *in silico* confirm the main points of pH-dependent regulatory mechanisms of electron transport in chloroplasts *in situ* discussed above.

4.3.1. Light-induced redox transients of PS1 electron acceptors and donors

Fig. 11 shows theoretical curves describing temporal patterns of relative concentrations of P_{700}^+ (top panel), oxidized ferredoxin, $NADP^+$, and plastoquinone (central panel), the light-induced changes in the lumen and stroma pH (pH_i and pH_o), and ATP concentration (bottom panel). The time-course of P_{700} photooxidation reveals a multiphase character, which is typical of experimental data for dark-adapted leaves (phases *A*, *B*, and *C*). The initial rise of $[P_{700}^+]$ to an intermediate level *A* is followed by a lag phase ($\Delta\tau$ ~5 s), which gives place to significant rise of $[P_{700}^+]$ toward a steady-state level (phases *B* and *C*). The time-course of P_{700} photooxidation correlates with non-monotonous changes in concentrations of $NADP^+$ and oxidized ferredoxin (Fd^+). Immediately after switching the light on, concentrations of $NADP^+$ and Fd^+ decrease (Fig. 11, central panel). Then NADPH and ferredoxin gradually re-oxidize due to the light-induced activation of the BBC cycle. Simultaneously with the rise of $[NADP^+]$ and $[Fd^+]$, one can notice a significant increase in $[P_{700}^+]$. These results are consistent with the notion that 'over-reduction' of PS1 electron acceptors during the induction phase is among the causes opposing P_{700} photooxidation [1].

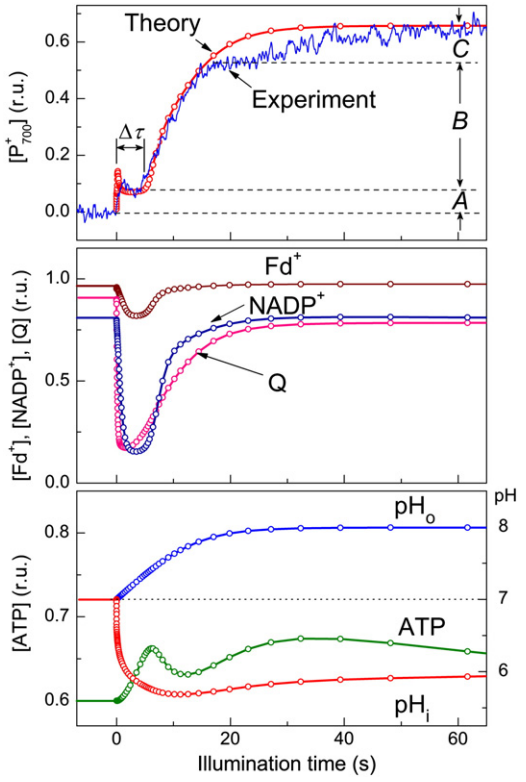

Fig. 11. Time-courses of variables $[P^{+}_{700}]$ (top panel), $[Fd^{+}]$, $[NADP^{+}]$ and [Q] (middle panel), kinetics of ATP concentration and light-induced pH changes in stroma (pH_o) and lumen (pH_i) (bottom panel). Concentrations of buffering groups in the lumen and stroma were taken as $B_i = 0.2$ mM ($pK_a = 6.0$) and $B_o = 25$ mM ($pK_a = 6.0$), respectively. Model parameters characterizing the capacities of mobile electron carriers Q, Pc, Fd, and NADP were as follows: $[Q]_0/[P_{700}]_0 = 10$, $[Pc]_0/[P_{700}]_0 = 1.5$, $[Fd]_0/[P_{700}]_0 = 8$, and $[NADP]_0/[P_{700}]_0 = 10$; $[ATP]_0/[P_{700}]_0 = 200$. In the initial state at the time moment $t = 0$, corresponding to dark-adapted chloroplasts, all P_{700} centers are reduced, 90% of plastoquinone, 95% of ferredoxin and 80% of NADP molecules were in the oxidized states. Experimental kinetics of redox transients of P_{700} in *Hibiscus rosa-sinensis* leaf (top panel) was registered after 10-min dark adaptation.

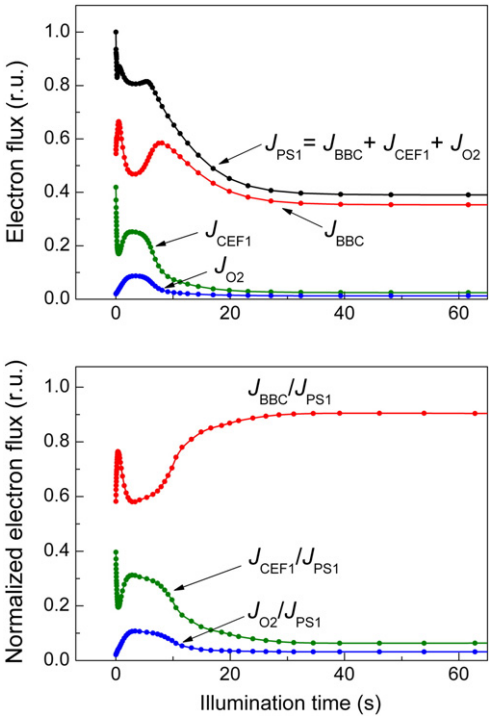

Fig. 12. Computed time-courses of electron fluxes on the PS1 acceptor side: J_{BBC} is the electron flux from ferredoxin to $NADP^{+}$; J_{CEF1} is the electron flux from ferredoxin to quinone, and J_{O2} is the electron flux from ferredoxin to oxygen (the Mehler reaction); J_{PS1} is the overall flux through PS1. Model parameters are the same as in Fig. 11.

The time-courses of pH_i, pH_o, and [ATP] are exemplified in the bottom panel of Fig. 11. The luminal pH_i shows the non-monotonous behavior. After the light-induced drop of pH_i, its value slightly increases toward a quasi-steady-state level $pH_i \approx 6$. This value is close to recent experimental estimates of pH_i in higher plant chloroplasts *in vitro* [84,85] and *in vivo* [71,86,87]. The stromal pH reaches $pH_o \approx 8$. This value is also close to experimental estimates [13,88,89]. The light-induced generation of the trans-thylakoid pH difference correlates with the net ATP synthesis. After a certain rise of ATP concentration, a level of ATP decreases due to its consumption in the activated BBC cycle.

Mathematical modeling enabled us to analyze the redistribution of electron fluxes on the acceptor side of PS1. Fig. 12 compares the temporal behaviors of the total electron flux through PS1 (J_{PS1}) and partial electron fluxes J_{BBC}, J_{CEF1}, and J_{O2}. Immediately after switching on the light, the calculated value of the total flux J_{PS1} drops. Initial phase of J_{PS1} decrease (Fig. 12) correlates with the initial phase of P_{700} photooxidation (Fig. 11). This is because the electron flux through PS1 is proportional to the product of P_{700} and Fd^{+} concentrations ($J_{PS1} \sim L_1 \cdot [P_{700}] \cdot [Fd^{+}]$, where L_1 is the light intensity, see for details Supplementary data). Therefore, the light-induced decrease in $[P_{700}]$ and $[Fd^{+}]$ would lead to a decrease in J_{PS1}. Then, after a lag phase, the electron flux through PS1 slowly decays toward a steady-state level. The light-induced decrease in pH_i causes a slowing down of QH_2 oxidation by the cytochrome b_6f-complex and an enhancement of energy losses in PS2. These processes are accompanied by re-oxidation of the plastoquinone pool (Fig. 11, central panel).

Note that the induction phase in the kinetics of P_{700} photooxidation (Fig. 11, top panel) correlates with the redistribution of electron fluxes on the acceptor side of PS1. During the lag phase, CEF1 and WWC give the marked contributions to electron flow in PS1 (Fig. 12, top panel). After the completion of the induction phase, CEF1 and WWC become insignificant, whereas the relative contribution of electron flow to the BBC cycle (J_{BBC}/J_{PS1}) increases (Fig. 12, bottom panel). This result is in agreement with the notion that CEF1 and WWC can serve as the starters for ATP synthesis on the initial stages of chloroplast illumination [5,7–10].

4.3.2. Effects of CO_2 and O_2 on electron fluxes and NPQ

Our model adequately describes effects of oxygen depletion on photosynthetic electron transport. In a good agreement with experiment, theory predicts that at ambient concentrations of CO_2 de-aeration of chloroplasts should be accompanied by dramatic decrease in a steady-state level of P^{+}_{700} (Fig. 5). Fig. 13 compares the results of computer simulation of the effects of CO_2 on LEF, pH_i, and pH_o under aerobic (21% O_2) or oxygen-deficient (2% O_2) conditions. As one could expect, electron flux through PS2 increases with the rise of atmospheric CO_2, reaching a steady-state level at $[CO_2] \geq 0.15\%$ (Fig. 13A). At sub-saturating concentrations of CO_2, just as in experiment, depletion of oxygen causes a decrease in J_{PS2}. The inhibitory effect of oxygen depletion disappears at saturating concentrations of CO_2. These results agree with experimental data (Fig. 10A), suggesting that the inhibition of electron outflow from PS1 to oxygen diminishes the overall rate of electron transfer through PS2.

As noted above, the down-regulation of LEF with lowering atmospheric CO_2 and depletion of oxygen can be explained by several reasons. These reasons are: *i*) impediments to electron transfer on the acceptor side of PS1, *ii*) deceleration of QH_2 oxidation caused by lowering the lumen pH_i, and *iii*) enhancement of energy losses in PS2 (NPQ↑). Results of numerical experiments presented in Fig. 13B support the mechanism of pH-dependent up- and down-regulation of

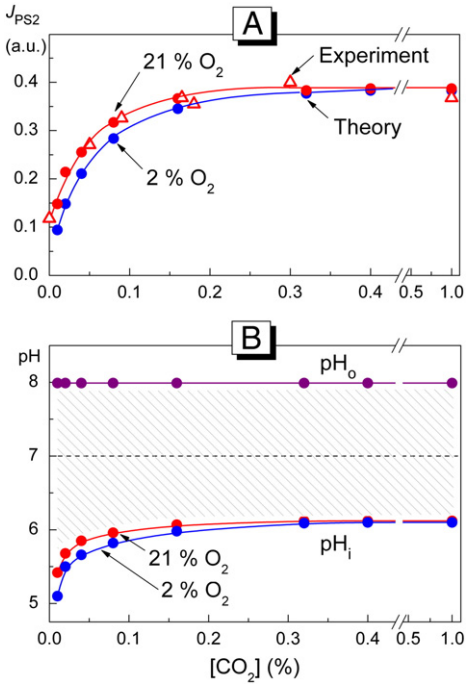

Fig. 13. Effect of CO_2 on steady-state electron flux through PS2, J_{PS2}, vs. the concentration of CO_2 computed for two concentrations of atmospheric O_2 (panel A). Computed value J_{PS2} is proportional to experimentally measured fluorescence parameter Φ_{PS2}. Open triangles show experimental points obtained for leaves exposed to air atmosphere with different concentrations of CO_2. Panel B shows the dependences of stationary pH values in the lumen (pH_i) and stroma (pH_o).

LEF. The model predicts that the thylakoid lumen becomes more acidic with decreasing the partial pressure of CO_2 (Fig. 13B). At ambient or low levels of CO_2, the depletion of oxygen causes additional decrease in pH_i (Fig. 13B), which manifests itself in experiment as an increase in NPQ (Fig. 10B).

5. Concluding remarks

In this work, we have investigated the short-term (~5–10 min) effects of atmospheric CO_2 and O_2 on induction events in *Hibiscus rosa-sinensis* leaves. These effects manifest themselves as multiphase kinetics of P_{700} redox transitions (Figs. 3 and 4) and non-monotonous changes in chlorophyll fluorescence parameters (Fig. 9). Depletion of CO_2 and O_2 causes a decrease in the rate of LEF (Fig. 10A) and dramatic lowering of P_{700}^{+} level (Fig. 5). These effects are explained by the impediment to electron efflux from PS1 at low acceptor capacity. With the release of the acceptor deficit, the rate of LEF increases and P_{700}^{+} level enhances. Atmospheric oxygen promotes the outflow of electrons from PS1, providing a rise of $[P_{700}^{+}]$ at ambient and low concentrations of CO_2 in air (≤0.06–0.08%). Similar effects were reported for leaves of other C_3 plants (e.g., *Spinacia oleracea* [68] and *Arabidopsis thaliana* [90]). A decrease in LEF upon depletion of CO_2 and O_2 is accompanied by significant (≥ 3-fold) rise of NPQ. This is in agreement with effects of CO_2 concentration and decreased O_2 concentration on induction fluorescence in leaves of other C_3 plants (*N. tabacum* [76,77], *Spinach oleracea* [91,92], *Pisum sativum* [93]).

Effects of atmospheric gases on electron transport are interrelated with pH-dependent regulation events in chloroplasts. Fig. 14 presents a general scheme of up- and down-regulation of electron transport processes associated with the light-induced changes in pH_i and pH_o. As noted above, a decrease in pH_i will impede electron flow between PS2 and PS1. The light-induced rise of pH_o can cause two opposite effects. An increase in pH_o will activate the BBC cycle reactions, thereby stimulating the efflux of electrons from PS1 to $NADP^+$. On the other hand, alkalization of stroma would retard the plastoquinone

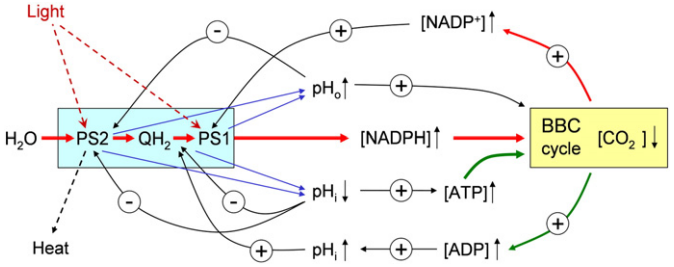

Fig. 14. A scheme illustrating a network of the negative (arrows marked by sign "minus") and positive (arrows marked by sign "plus") feedback control mechanisms in photosynthetic chain of electron transport. Up and down vertical arrows symbolize an increase or decrease in metabolite concentrations, respectively.

reduction by PS2, thereby diminishing the electron flow from PS2 to PS1. At low PS1 acceptor capacity (low $[CO_2]$ and $[O_2]$), a decrease in LEF will lessen the ATP consumption in the BBC cycle. In this case, the proton drain from the lumen through the ATP synthases becomes slower. Therefore, the light-induced decrease in pH_i will be more significant at low concentrations of CO_2 (Fig. 13B). This explains why NPQ increases with depletion of CO_2 in air (Fig. 10). At first sight, this mechanism is somewhat similar to type II flexibility mechanism suggested in [7–10]. It should be noted, however, that we can explain the reciprocal behavior of fluorescence parameters Φ_{PS2} and q_{NPQ} (Fig. 10) without the implication of flexible H^+/ATP stoichiometry.

Mathematical modeling of electron and proton transport in chloroplasts supports the above interpretation of experimental data in the context of pH-dependent control of electron transport processes. Our model shows how the interplay of positive and negative feedback reactions (Fig. 14) manifests itself in multiphase patterns of P_{700} redox transients (Fig. 11). The model predicts the reciprocal changes in LEF and NPQ upon depletion of CO_2 and O_2. A relative contribution of LEF to electron flow through PS1 (J_{BBC}/J_{PS1}) increases during the induction phase, while alternative electron fluxes (CEF1 and WWC) become weakened (Fig. 12). This result is consistent with experimental evidence that in C_3 plants CEF1 is insignificant under the steady-state conditions.

Acknowledgements

This work was supported partly by grant 09-04-00978a from the Russian Foundation for Basic Researches. Authors are grateful to A.V. Sokolov, A.K. Petrov, I.A. and V.A. Kot for their advices about using gas sensors.

Appendix A. Supplementary data

Supplementary data to this article can be found online at doi:10.1016/j.bbabio.2010.12.012.

References

[1] G. Edwards, D.A. Walker, C_3, C_4: mechanisms, and cellular and environmental regulation of photosynthesis, Blackwell, Oxford, 1983.
[2] G. Noctor, C.H. Foyer, Homeostasis of adenylate status during photosynthesis in a fluctuating environment, J. Exp. Botany 51 (2000) 347–356.
[3] A. Haldrup, P.E. Jensen, C. Lunde, H.V. Scheller, Balance of power: a view of the mechanism of photosynthetic state transitions, Trends Plant Sci. 6 (2001) 301–305.
[4] J.F. Allen, State transitions—a question of balance, Science 299 (2003) 1530–1532.
[5] J.F. Allen, Cyclic, pseudocyclic and noncyclic photophosphorylation: new links in the chain, Trends Plant Sci. 8 (2003) 15–19.
[6] T. Pfannschmidt, Chloroplast redox signals: how photosynthesis controls its own genes, Trends Plant Sci. 8 (2003) 33–41.
[7] D.M. Kramer, C.A. Sacksteder, J.A. Cruz, Balancing the central roles of the thylakoid proton gradient, Trends Plant Sci. 8 (2003) 27–32.
[8] D.M. Kramer, T.J. Avenson, G.E. Edwards, Dynamic flexibility in the light reactions of photosynthesis governed by both electron and proton transfer reactions, Trends Plant. Sci. 9 (2004) 349–357.

[9] E. Kanervo, M. Suirsa, E.-M. Aro, Functional flexibility and acclimation of the thylakoid membrane, Photochem. Photobiol. Sci. 4 (2005) 1072–1080.
[10] J.A. Cruz, T.J. Avenson, A. Kanazawa, K. Takizawa, G.E. Edwards, D.M. Kramer, Plasticity in light reactions of photosynthesis for energy production and photoprotection, J. Exp. Botany 56 (2007) 395–406.
[11] N.R. Baker, J. Harbinson, D.M. Kramer, Determining the limitations and regulation of photosynthetic energy transduction in leaves, Plant, Cell & Environment 30 (2007) 1107–1125.
[12] Z. Li, S. Wakao, B.B. Fischer, K.K. Niyogi, Sensing and responding to excess light, Annu. Rev. Plant Biol. 60 (2009) 239–260.
[13] K. Werdan, H.V. Heldt, M. Milovancev, The role of pH in the regulation of carbon fixation in the chloroplast stroma. Studies on CO_2 fixation in the light and dark, Biochim. Biophys. Acta 396 (1975) 276–292.
[14] K.A. Mott, J.A. Berry, Effects of pH on activity and activation of ribulose 1, 5-biphosphate carboxylase at air level CO2, Plant Physiol. 82 (1986) 77–82.
[15] I. Andersson, Catalysis and regulation in Rubisco, J. Exp. Botany 59 (2008) 1555–1568.
[16] R.F. Sage, Y.-P. Cen, M. Li, The activation state of rubisco directly limits photosynthesis at low CO_2 and low O_2 partial pressure, Photosyn. Res. 71 (2002) 241–250.
[17] D.S. Bendall, R.S. Manasse, Cyclic photophosorylation and electron transport, Biochim. Biophys. Acta 1229 (1995) 23–38.
[18] P. Joliot, A. Joliot, Cyclic electron transfer in plant leaf, Proc. Natl. Acad. Sci. USA 99 (2002) 10209–10214.
[19] T. Joët, L. Cournac, G. Peltier, M. Havaux, Cyclic electron flow around photosystem I in C_3 plants. In vivo control by the redox state of chloroplasts and involvement of the NADH-dehydrogenase complex, Plant Physiol. 128 (2002) 760–769.
[20] Y. Munekage, M. Hashimoto, C. Miyake, K.-I. Tomizawa, T. Endo, M. Tasaka, T. Shikanai, Cyclic electron flow around photosystem I is essential for photosynthesis, Nature 429 (2004) 579–582.
[21] G.N. Johnson, Cyclic electron transport in C_3 plants: fact or artefact? J. Exp. Bot. 56 (2005) 407–416.
[22] P. Joliot, A. Joliot, Quantification of cyclic and linear flows in plants, Proc. Natl. Acad. Sci. USA 102 (2005) 4913–4918.
[23] M. Iwai, K. Takizawa, R. Tokutsu, A. Okamuro, Y. Takahashi, J. Minagawa, Isolation of the elusive supercomplex that drives cyclic electron flow in photosynthesis, Nature 464 (2010) 1210–1214.
[24] J.E. Backhausen, C. Kitzmann, P. Horton, R. Scheibe, Electron acceptors in isolated intact spinach chloroplasts act hierarchically to prevent over-reduction and competition for electrons, Photosynth. Res. 64 (2000) 1–13.
[25] K. Asada, The water–water cycle in chloroplasts: scavenging of active oxygen and dissipation of excess photons, Annu. Rev. Plant Physiol. Plant Mol. Biol. 50 (1999) 601–639.
[26] U. Heber, Irrungen, wirrungen? The Mehler reaction in relation to cyclic electron transport in C_3 plants, Photosynth. Res. 73 (2002) 223–231.
[27] M.R. Badger, S. von Caemmerer, S. Ruuska, H. Nakano, Electron flow to oxygen in higher plants and algae: rates and control of direct photoreduction (Mehler reaction) and rubisco oxygenase, Philos. Trans. R. Soc. Lond. B 355 (2000) 1433–1446.
[28] D.R. Ort, N.R. Baker, A photoprotective role for O_2 as an alternative electron sink in photosynthesis? Curr. Opp. Plant Biol. 5 (2002) 193–197.
[29] D. Rumeau, G. Peltier, L. Cournac, Chlororespiration and cyclic electron flow around PSI during photosynthesis and plant stress response, Plant, Cell & Environ. 30 (2007) 1041–1051.
[30] H.H. Stiehl, H.T. Witt, Quantitative treatment of the function of plastoquinone in photosynthesis, Z. Naturforsch. Teil B 24 (1969) 1588–1598.
[31] B. Rumberg, U. Siggel, pH changes in the inner phase of the thylakoids during photosynthesis, Naturwissenschaften 56 (1969) 130–132.
[32] A.N. Tikhonov, G.B. Khomutov, E.K. Ruuge, L.A. Blumenfeld, Electron transport control in chloroplasts. Effects of photosynthetic control monitored by the intrathylakoid pH, Biochim. Biophys. Acta 637 (1981) 321–333.
[33] A.N. Tikhonov, G.B. Khomutov, E.K. Ruuge, Electron transport control in chloroplasts. Effects of magnesium ions on the electron flow between two photosystems, Photobiochem. Photobiophys. 8 (1984) 261–269.
[34] C. Sigalat, F. Haraux, Y. de Kouchkovsky, Flow-force relationships in lettuce thylakoids. 1. Strict control of electron flow by internal pH, Biochemistry 32 (1993) 10193–10200.
[35] L.A. Blumenfeld, A.N. Tikhonov, Biophysical Thermodynamics of Intracellular Processes, Molecular Machines of the Living Cell, Springer, New York, 1994, pp. 112–173.
[36] D.M. Kramer, C.A. Sacksteder, J.A. Cruz, How acidic is the lumen? Photosynth. Res. 60 (1999) 151–163.
[37] K. Maxwell, G.N. Johnson, Chlorophyll fluorescence: a practical guide, J. Exp. Botany 51 (2000) 659–668.
[38] P. Müller, X.-P. Li, K.K. Niyogi, Non-photochemical quenching. A response to excess light energy, Plant Physiol. 125 (2001) 1558–1566.
[39] X.-P. Li, A.M. Gilmore, S. Caffarri, R. Bassi, T. Golan, D. Kramer, K.K. Niyogi, Regulation of photosynthetic light harvesting involves intrathylakoid lumen pH sensing by the PsbS protein, J. Biol. Chem. 279 (2004) 22866–22874.
[40] N. Baker, Chlorophyll fluorescence: a probe of photosynthesis *in vivo*, Annu. Rev. Plant Biol. 59 (2008) 89–113.
[41] S.I. Allakhverdiev, V.D. Kreslavski, V.V. Klimov, D.A. Los, R. Carpentier, P. Mohanty, Heat stress: an overview of molecular responses in photosynthesis, Photosynth. Res. 98 (2008) 541–550.
[42] K. Tagawa, H.Y. Tsuimoto, D. Arnon, Analysis of photosynthetic reactions by the use of monochromatic light, Nature 199 (1963) 1247–1252.
[43] Y. Kobayashi, U. Heber, Rates of vectorial proton transport supported by cyclic electron flow during oxygen reduction by illuminated intact chloroplasts, Photosynth. Res. 41 (1994) 419–428.
[44] G. Peltier, L. Cournac, Chlororespiration, Annu. Rev. Plant Biol. 53 (2002) 523–550.
[45] R.F. Sage, Y.-P. Cen, M. Li, The activation state of rubisco directly limits photosynthesis at low CO_2 and low O_2 partial pressure, Photosynth. Res. 71 (2002) 241–250.
[46] a) G. Cornic, J.-M. Briantais, Partitioning of photosynthetic electron flow between CO_2 and O_2 reduction in a C_3 leaf (*Phaseolus vulgaris* L.) at different CO_2 concentrations and during drought stress, Planta 183 (1991) 178–1848;
b) A.J. Golding, G.N. Johnson, Down-regulation of linear and activation of cyclic electron transport during drought, Planta 218 (2003) 107–114.
[47] B.B. Buchanan, Regulation of CO_2 assimilation in oxygenic photosynthesis: the ferredoxin/thioredoxin system. Perspective on its discovery, present status, and future development, Arch. Biochem. Biophys. 288 (1991) 1–9.
[48] G.R. Hendrey, S.P. Long, I.F. McKee, N.R. Baker, Can photosynthesis respond to short-term fluctuations in atmospheric carbon dioxide? Photosynth. Res. 51 (1997) 179–184.
[49] W.S. Chow, A.B. Hope, Electron fluxes through photosystem I in cucumber leaf discs probed by far-red light, Photosynth. Res. 81 (2004) 77–89.
[50] I.V. Kuvykin, A.V. Vershubskii, V.V. Ptushenko, A.N. Tikhonov, Oxygen as an alternative acceptor in the photosynthetic electron transfer chain in C_3 plants, Biochemistry (Moscow) 73 (2008) 1063–1075.
[51] B.V. Trubitsin, M.D. Mamedov, L.A. Vitukhnovskaya, A.Yu. Semenov, A.N. Tikhonov, EPR study of light-induced regulation of photosynthetic electron transport in *Synechocystis* sp. strain PCC 6803, FEBS Letters 544 (2003) 15–20.
[52] B.V. Trubitsin, V.V. Ptushenko, O.A. Koksharova, M.D. Mamedov, L.A. Vitukhnovskaya, I.A. Grigor'ev, A.Yu. Semenov, A.N. Tikhonov, EPR study of electron transport in the cyanobacterium *Synechocystis* sp. PCC 6803. Oxygen-dependent interrelations between photosynthetic and respiratory electron transport chains, Biochim. Biophys. Acta 1708 (2005) 238–249.
[53] E. Rabinovitch, Photosynthesis and Related Processes. 1956. V. II, part 2.
[54] K. Oxborough, N.R. Baker, Resolving chlorophyll a fluorescence images of photosynthetic efficiency into photochemical and non-photochemical components—calculation of qP and F_v'/F_m' without measuring F_o', Photosynth. Res. 54 (1997) 135–142.
[55] A.Yu. Dubinskii, A.N. Tikhonov, Regulation of electron and proton transport in the chloroplasts. Kinetic model and comparison of it with the experiment, Biophysics 39 (1994) 657–670.
[56] A.Yu. Dubinskii, A.N. Tikhonov, Mathematical simulation of the light-induced uptake of protons by chloroplasts upon various mechanisms of proton leak through the thylakoid membrane, Biophysics 40 (1995) 341–347.
[57] A.Yu. Dubinskii, A.N. Tikhonov, Mathemetical model of thylakoid as the distributed heterogeneous system of electron and proton transport, Biophysics 42 (1997) 644–660.
[58] A.V. Vershubskii, V.I. Priklonskii, A.N. Tikhonov, Electron and proton transport in chloroplasts: a mathematical model constructed with regard for the lateral heterogeneity of thylakoids, Biophysics 46 (2001) 448–457.
[59] A.V. Vershubskii, V.I. Priklonskii, A.N. Tikhonov, Mathematical modeling of electron and proton transport coupled with ATP synthesis in chloroplasts, Biophysics 49 (2004) 52–65.
[60] A.V. Vershubskii, V.I. Priklonskii, A.N. Tikhonov, Effects of diffusion and topological factors on the efficiency of energy coupling in chloroplasts with heterogeneous partitioning of protein complexes in thylakoids of grana and stroma. A mathematical model, Biochemistry (Moscow) 69 (2004) 1016–1024.
[61] A.V. Vershubskii, V.I. Priklonskii, A.N. Tikhonov, Kinetic model for electron and proton transport in chloroplasts with nonuniform distribution of protein complexes in thylakoid membranes, Russian J. Phys. Chem. 80 (2006) 467–474.
[62] A.E. Frolov, A.N. Tikhonov, Influence of light-induced changes in stromal and lumenal pH on electron transport kinetics in chloroplasts: mathematical modeling, Biophysics 52 (2007) 398–405.
[63] I.V. Kuvykin, A.V. Vershubskii, A.N. Tikhonov, Alternative routes of photoinduced electron transport in chloroplasts, Russian J. Phys. Chem. B 3 (2009) 230–241.
[64] I.V. Kuvykin, A.V. Vershubskii, V.I. Priklonskii, A.N. Tikhonov, Computer simulation study of pH-dependent regulation of electron transport in chloroplasts, Biophysics 54 (2009) 455–464.
[65] A.V. Vershubskii, I.V. Kuvykin, V.I. Priklonskii, A.N. Tikhonov, Functional and topological aspects of pH-dependent regulation of electron and proton transport in chloroplasts in silico, BioSystems 103 (2011) 164–179.
[66] T.D. Sharkey, C.J. Bernacchi, G.D. Farquhar, E.L. Singsaas, Fitting photosynthetic carbon dioxide response curves for C_3 leaves, Plant, Cell & Environ. 30 (2007) 1035–1040.
[67] A.N. Webber, W. Lubitz, P700: the primary electron donor of photosystem I, Biochim. Biophys. Acta 1507 (2001) 61–79.
[68] U. Heber, S. Neimanis, K. Siebke, G. Schönknecht, E. Katona, Chloroplast energization and oxidation of P_{700}/plastocyanin in illuminated leaves at reduced level of CO_2 or oxygen, Photosynth. Res. 34 (1992) 433–447.
[69] B. Ivanov, Y. Kobayashi, N.G. Bukhov, U. Heber, Photosystem I-dependent cyclic electron flow in intact spinach chloroplasts: occurrence dependence on redox conditions and electron acceptors and inhibition by antimycin A, Photosynth. Res. 57 (1998) 61–70.
[70] C. Breyton, B. Nandha, G. Johnson, P. Joliot, G. Finazzi, Redox modulation of cyclic electron flow around photosystem I in C3 plants, Biochemistry 45 (2006) 13465–13475.
[71] S.B. Ryzhikov, A.N. Tikhonov, Regulation of electron transfer in photosynthetic membranes of higher plants, Biophysics 33 (1988) 642–646.

[72] O. Björkman, B. Demmig, Photon yield of O_2 evolution and chlorophyll fluorescence characteristics at 77 K among vascular plants of diverse origins, Planta 170 (1987) 489–504.
[73] G.N. Johnson, A.J. Young, J.D. Scholes, P. Horton, The dissipation of excess excitation energy in British plant species, Plant, Cell & Environ. 16 (1993) 673–679.
[74] V.A. Karavaev, A.K. Kukushkin, Adaptation to the dark and far red light of the leaves of higher plants in conditions of oxygen lack, Biophysics 20 (1975) 86–91.
[75] D. Lazar, Chlorophyll a fluorescence induction, Biochim. Biophys. Acta 1412 (1999) 1–28.
[76] A. Kanazawa, D.M. Kramer, In vivo modulation of non-photochemical exciton quenching (NPQ) by regulation of the chloroplast ATP synthase, Proc. Natl. Acad. Sci. USA 99 (2002) 12789–12794.
[77] T.J. Avenson, J.A. Cruz, D.M. Kramer, Modulation of energy dependent quenching of excitons in antenna of higher plants, Proc. Natl. Acad. Sci. USA 101 (2004) 5530–5535.
[78] A. Ligeza, A. Wisniewska, W.K. Subczynski, A.N. Tikhonov, Oxygen production and consumption by chloroplasts in situ and in vitro as studied with microscopic spin label probes, Biochim. Biophys. Acta 1186 (1994) 201–208.
[79] A. Ligeza, A.N. Tikhonov, W.K. Subczynski, In situ measurements of oxygen production and consumption using paramagnetic fusinite particles injected into a bean leaf, Biochim. Biophys. Acta 1319 (1997) 133–137.
[80] M.R. Roussel, A.U. Igamberdiev, Dynamics and mechanisms of oscillatory photosynthesis, BioSystems 103 (2011) 230–238.
[81] I.E. Woodrow, J.A. Berry, Enzymatic regulation of photosynthetic CO_2 fixation in C_3 plants, Annu. Rev. Plant Physiol. Plant Mol. Biol. 39 (1988) 533–594.
[82] R.G. Jensen, J.T. Bahr, Ribulose 1,5-bisphosphate carboxylase-oxygenase, Annu. Rev. Plant Physiol. 28 (1977) 379–400.
[83] R.W. Pickersgill, An upper limit to the active site concentration of ribulose bisphosphate carboxylase in chloroplasts, Biochem. J. 236 (1986) 311.
[84] B.V. Trubitsin, A.N. Tikhonov, Determination of a transmembrane pH difference in chloroplasts with a spin label tempamine, J. Magn. Res. 163 (2003) 257–269.
[85] A.N. Tikhonov, R.V. Agafonov, I.A. Grigor'ev, I.A. Kirilyuk, V.V. Ptushenko, B.V. Trubitsin, Spin-probes designed for measuring the intrathylakoid pH in chloroplasts, Biochim. Biophis. Acta 1777 (2008) 285–294.
[86] J.N. Nishio, J. Whimarsh, Dissipation of the proton electrochemical potential in intact chloroplasts. II. The pH gradient monitored by cytochrome *f* reduction kinetics, Plant Physiol. 101 (1994) 89–96.
[87] K. Takizawa, J.A. Cruz, A. Kanazawa, D.M. Kramer, The thylakoid proton motive force in vivo. Quantitative, non-invasive probes, energetics, and regulatory consequences of light-induced pmf, Biochim. Biophys. Acta 1767 (2007) 1233–1244.
[88] H.W. Heldt, K. Werdan, M. Milivancev, G. Geller, Alkalization of the chloroplast stroma caused by light-dependent proton flux into the thylakoid space, Biochim. Biophis. Acta 314 (1973) 224–241.
[89] S.P. Robinson, The involvement of stromal ATP in maintaining the pH gradient across the chloroplast envelope in the light, Biochim. Biophis. Acta 806 (1985) 187–194.
[90] M. Tsuyama, Y. Kobayashi, Reduction of the primary donor P700 of photosystem I during steady-state photosynthesis under low light in *Arabidopsis*, Photosynth. Res. 99 (2009) 37–47.
[91] M.N. Sivak, D.A. Walker, Some effects of CO_2 concentration and decreased O_2 concentration on induction fluorescence in leaves, Proc. R. Soc. Lond. B 217 (1983) 377–392.
[92] M.N. Sivak, R.T. Prinsley, D.A. Walker, Some effects of changes in gas phase on the steady-state chlorophyll a fluorescence exhibited by illuminated leaves, Proc. R. Soc. Lond. B 217 (1983) 393–404.
[93] M. Bradbury, C.R. Ireland, N.R. Baker, An analysis of the chlorophyll-fluorescence transients from pea leaves generated by changes in atmospheric concentrations of CO_2 and O_2, Biochim. Biophis. Acta 806 (1985) 357–365.